www.ptcer.pl/mccm

MATERIAŁY CERAMICZNE /CERAMIC MATERIALS/, 63, 1, (2011), 109-116

Dense and Porous Zirconia Prepared by Gelatine and Agar Gel-Casting: Microstructural and Mechanical Characterization

Jean-Marc Tulliani[1], Cecilia Bartuli[2], Edoardo Bemporad[3], Alessio Cavalieri[1], Jacopo Tirillò[2], Giovanni Pulci[2], Marco Sebastiani[3]

[1] Dip. di Scienza dei Materiali e Ingegneria Chimica, Politecnico di Torino, Torino, Italy
[2] Dip. di Ingegneria Chimica Materiali Ambiente, Sapienza Università di Roma, Roma, Italy
[3] Dip. di Ingegneria Meccanica e Industriale, Università di Roma Tre, Roma, Italy
e-mail: jeanmarc.tulliani@polito.it

Abstract

Dense and cellular yttria-tetragonal zirconia polycrystal (Y-TZP) bodies were produced by using a natural gelatine and two different agars as gelling agents, while commercial polyethylene (PE) spheres were added (125 to 300 μm diameter) as a volatile pore forming agent to create 50-65 vol.% spherical macro-pores, uniformly distributed in a micro-porous matrix. The microstructure of all dense and cellular ceramics was characterized by FEG-SEM and Focused Ion Beam (FIB) techniques. The mechanical properties of both dense and porous samples were investigated at the microscale by nanoindentation testing, while the influence of microporosity was obtained by the analysis of hardness and modulus depth profiles, coupled with FIB-SEM section observations of selected indentation marks. Mechanical characterization at the macroscale consisted of uniaxial compression tests and four point bending tests.

Keywords: Gel-casting, Scanning electron microscopy, Porosity, Mechanical properties, ZrO_2

GĘSTE I POROWATE TWORZYWA CYRKONIOWE WYTWORZONE METODĄ ODLEWANIA ŻELOWEGO ŻELATYNOWEGO I AGAROWEGO: CHARAKTERYSTYKA MIKROSTRUKTURALNA I MECHANICZNA

Wytworzono gęste i komórkowe polikrystaliczne materiały tlenku cyrkonu stabilizowanego tlenkiem itru, wykorzystując naturalną żelatynę i dwa rodzaje agarozy, jako czynniki żelujące, przy czym komercyjne kule polietylenowe (PE) o średnicach 125 do 300 μm dodano, jako lotny czynnik porotwórczy, aby wytworzyć 50-65 % obj. kulistych makroporów rozproszonych równomiernie w mikroporowatej osnowie. Mikrostrukturę otrzymanej ceramiki, zarówno gęstej jak i komórkowej, scharakteryzowano za pomocą technik FEG-SEM i zogniskowanej wiązki jonów (*focused ion beam*, FIB). Właściwości mechaniczne, zarówno gęstych jak i porowatych próbek, określono w mikroskali za pomocą badania nanoodcisków (*nanoindentation testing*), natomiast wpływ mikroporowatości uzyskano na podstawie analizy profili głębokościowych twardości i modułu w połączeniu z obserwacjami SEM wybranych odcisków na przekrojach otrzymanych za pomocą FIB. Charakterystyka mechaniczna w makroskali objęła testy jednoosiowego ściskania i czteropunktowego zginania.

Słowa kluczowe: odlewanie żelowe, skaningowa mikroskopia elektronowa, porowatość, właściwości mechaniczne, ZrO_2

1. Introduction

A variety of applications, such as, for example, molten metals filtration, high-temperature thermal insulation, support for catalytic reactions, filtration of particulates from diesel engine exhaust gases and of hot corrosive gases in various industrial processes and bone substitutes require porous ceramics, thus their interest has rapidly grown over the last decades [1, 2]. The porous features influence the properties of the produced components, thus two crucial steps are involved in the production of cellular materials: first, the selection and set-up of a reliable forming method allowing a strict control of pore size, volume, distribution and morphology; second, a proper characterization of the actual porosity features as well as of the mechanical/functional performances [1, 2].

This paper deals mostly with the exploitation of a modified gel-casting process to develop dense and porous materials, having controlled porosity features. Gel-casting is a well-known wet forming method based on the combination of ceramic processing and polymer chemistry: a ceramic powder is dispersed into a monomer solution, prior to casting into a non-porous mould and the polymerization is then promoted. As a consequence, ceramic particles are entrapped into the rigid and homogenous polymeric network [3]. After gel formation, gel-cast green materials can be easily demoulded and are then dried in controlled conditions. The produced green bodies are characterized by high strength, allowing their machinability, and a low amount of organic additives, avoiding a preliminary thermal treatment as in the injection moulding process [4]. The technique is also versatile and has been extended to a variety of ceramic materials, such as, for example: Al_2O_3 [3-6], Si_3N_4 [7], hydroxy apatite [8], SiC/Si_3N_4 composites [9], ZrO_2 [10] and mullite [11].

Different monomers were exploited for gel-casting, starting from acrylamide systems [3, 4, 9, 12], now withdrawn due

to their neurotoxicity [5], as well as alternative gelling agents, such as, for example, agar [6] and its purified derivative, agarose [6, 7, 10, 13], carrageenan gums [13], egg white [14], gelatine [15-17], sodium alginate [18], glycerol [8] and polyvinyl alcohol [17]. Natural gelling agents present the advantages of a polymerization just promoted by cooling below the glass-transition temperature, without the use of a catalyst and an initiator, as synthetic monomers do, and of a low environmental impact. In the present work a natural gelatine, precisely a pig-derived product for food industry, was used, as well as agar, which is derived from the red algae class of seaweed by a series of extraction and bleaching operations [19].

The gel-casting process was firstly set-up for preparing dense components, and more recently modified to fabricate also porous ceramics, by combining it with foaming techniques, or replica methods, or even the addition of a sacrificial phase [1, 9, 10, 20]. In this work, a fugitive phase, made of commercial polyethylene spheres in a size range selected by sieving, was added to the ceramic suspension before gelling. The shape, size and size distribution of these spheres as well as their volume fraction with respect to the ceramic content into the slurry can allow a strict control of many porosity features of the final components. The feasibility of the process was demonstrated by developing porous components with a pore volume percentage around 40-50 %.

2. Experimental

Commercial stabilized zirconia with 3 mol.% of yttria (yttria tetragonal zirconia polycrystal, Y-TZP, grade TZ-3YS supplied by Tosoh Co., Japan) was used for the preparation of ceramic suspensions. Particle size distribution was determined by means of a laser granulometer (Fristch analysette 22) in ethanol after 10 minutes of ultrasonication: the mean diameter of the zirconia powder was about 0.6 micron and the diameters corresponding to 10 % and 90 % of the particle size distributions were respectively 0.33 and 1.1 micron. In the first step dense components were produced to set-up the procedure.

A pig skin-derived gelatine, produced by Italgelatine (Italy), was chosen as a gelling agent: its melting point is 32.5°C and its viscosity in aqueous solution (6.67 wt%) at 60°C is 42.5 mPa·s with a related pH of 5.08. This gelatine calcined up to 550°C for 18 hours yielded a limited amount of residual ashes (0.2 wt% of the starting mass), as confirmed by the thermogravimetric analysis [21]. For the suspensions preparation, the gelatine was dissolved into deionized water at 60°C and this solution was then added to the ceramic suspensions at the same temperature under stirring, so that an amount of gelling agent of 3 wt%, with respect to the final water content, was reached. Then, ceramic suspensions had a final solid loading of 60 wt%. The powder was dispersed into water at natural pH, prior to gelatine addition, and sonicated for 10 minutes [22].

Two different kinds of agar were chosen as gelling agents: gum agar, Fluka 05040 and Sigma-Aldrich 07049. After calcination, the residual ash fraction were equal to around 3.9 wt% and 0.8 wt%, respectively, for the Fluka and Sigma agar, estimated on a pellet of both pure agar which was uniaxially pressed at 100 MPa and heated up to 600°C for 2 hours. With the Fluka agar, suspensions having a content of 55.35 wt% were prepared in deionized water and Dolapix PC 33 (Zschimmer & Schwarz, 1.22 wt% respect to zirconia powder) was added as a dispersant, while with the Sigma-Aldrich agar, suspensions having a higher solid content of 58.82 wt% could be prepared in deionized water, keeping constant the Dolapix PC 33 content. Part of the water was used to disperse the zirconia powder with Dolapix by means of a magnetic stirrer for 10 minutes and after that, with an ultrasonic probe for 15 minutes. The agars were dissolved into the remaining part of the deionised water at 90°C for 1 hour and the solutions were then cooled down to 60°C and added to the ceramic suspensions, which were, in the meantime, warmed at the same temperature under magnetic stirring. Several tests were carried out to determine the optimal agar amount: starting from 1 wt% and reducing its content down to 0.74 wt%, with respect to water.

Gelatine and agar tend to make foam under stirring, a well known phenomenon for organic materials but also with water soluble polymers belonging to the acrylamide family [11]. Then, suspensions containing the gelatine and the Fluka agar were cast under vacuum (at about 10^{-2} Pa), while to those containing the Sigma agar, due to their lower viscosity, some drops of poly(ethylene) glycol (PEG) were added as an antifoaming agent, prior to casting into Plexiglas moulds at about 50°C (Fig. 1). In this case, no de-airing step was performed, except that the moulds were tapped twenty times to remove incidental air bubbles entrapped into the ceramic suspensions. The chosen casting temperature represented a good compromise between the low viscosity necessary for suspensions casting and the agar gelling point (36°C). The suspensions viscosity was determined by means of a Brookfield DVII+ viscosimeter with an ULA-EY UL adapter for the measurement of low viscosities liquids. Cylindrical moulds having different dimensions (internal diameter from 12 up to

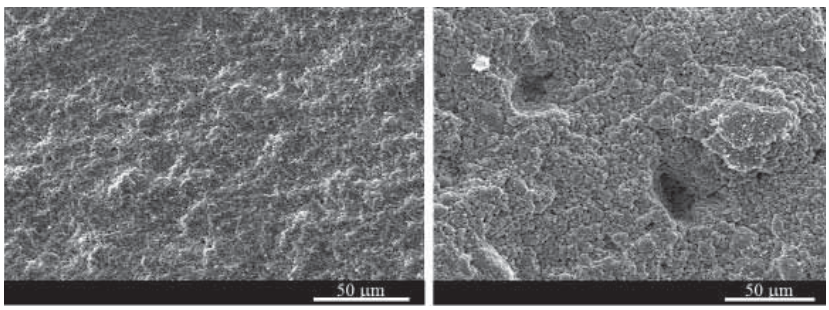

Fig. 1. SEM micrograph of a fracture surface of two sintered samples: a) w/o PEG addition, b) after PEG addition.

18 mm and height in the range 30 - 55 mm) were used for all the samples, while bars (10 × 12 × 94 mm^3) were employed only with the samples made from agar. In the first moment, the cast samples were slowly dried at room temperature under controlled humid atmosphere and then, after demoulding, in static air. Complete drying of the samples required 2 to more than 3 weeks: agar samples could be dehydrated faster than the gelatine ones.

A polyethylene (PE) powder, supplied by Clariant Italia SpA, having a density at 23°C of about 0.92 - 0.94 g/cm^3 was used as a fugitive phase. Its thermal decomposition is almost completed after calcination at 550°C [23]. PE powder, firstly sieved in the range 125–300 μm before dispersion into ceramic suspensions, was made of almost spherical particles, but irregular structures were also present [24]. To fabricate porous ceramics, PE spheres were dispersed in water, in suitable amounts to obtain zirconia suspensions having 50 vol.% or 65 vol.% polymers, leading to the samples labelled, from now on, P50 and P65, respectively. With gelatine addition, the ceramic content of the slurries in the samples P50 was the same as for the dense samples, while with agar it was slightly lower with respect to the dense materials (55.2 wt%), to keep a suitable viscosity of the suspension for casting. On the contrary, the gelling agent content was kept constant with water fraction and was the same as for the dense samples.

Dense gel-cast zirconia ceramics were sintered at 1550°C (heating rate of 1°C/min, soaking time of 2 hours at 600°C, to completely decompose the gelling agent, and then, at another heating rate of 1°C/min to the maximum temperature for 1 or 2 hours and cooling rate of 5°C/min down to room temperature). The sintering cycle was set-up on the ground of porosimetric studies performed on gel-cast bars (Carlo Erba 2000 porosimeter) [23]. A huge shrinkage (ca. 40 %) between the green humid samples and the sintered ones was observed.

Another difference between dense and porous samples consisted in the modification of the overall thermal cycle during heating up to 450°C: various intermediate steps, on the basis of the TGA results [21], have to be introduced to control the thermal decomposition of the polyethylene spheres, without collapsing of the structure. Then, the following firing cycle was adopted: a constant heating ramp of 1°C/min, with the first soaking time of 10 hours at 230°C, the second plateau at 300°C for 2 hours, followed by the third one at 450°C for 2 hours and the last one at 600°C for 2 hours.

The images of porous samples were acquired by Optical Microscopy (2560 × 1920 pixel resolution) and processed using a cascade of filters (contrast equalization, threshold, binarization, mean, ranking, morphological closing), by the use of the SIS commercial software for the digital image analysis. The detected voids were then classified on the basis of their area and the shape factor was then calculated.

Nanoindentation testing was performed by means of a Berkovich diamond indenter, using an Agilent G200 Nano Indenter, in a continuous stiffness measurement mode (CSM) under a constant strain rate of 0.05 s^{-1} and a maximum load of 650 mN (other test and fitting parameters were chosen according to ISO 14577-1-2 standards). In the case of the adopted CSM method, the contact stiffness is dynamically measured during indentation, as the indenter is driven in during loading, and continuous Hardness/depth and Modulus/depth curves were then obtained by the use of the following equations [26]:

$$H = \frac{P}{A}, \tag{1}$$

$$E_r = \frac{\sqrt{\pi}}{2\beta} \cdot \frac{S}{\sqrt{A}}. \tag{2}$$

$S = dP/dh$ is the elastic contact stiffness which is evaluated, after fitting the upper portion (usually 50 %) of the unloading curve to a power-law relation (Oliver-Pharr method, [26]), as the slope of the unloading curve at maximum load Pmax. β is a numerical factor equal to 1.034 for a Berkovich indenter, related to a lack of symmetry of the indenter [27]. In the present work a value of 1.000 was adopted, as suggested by the ISO 14577-1-2 standard. The elastic modulus of the tested samples can then be estimated by equation (3):

$$\frac{1}{E_r} = \frac{(1-\nu)^2}{E} + \frac{(1-\nu_i)^2}{E_i}, \tag{3}$$

where E_i and ν_i are, respectively, the elastic modulus and the Poisson ratio of the indenter. The reliable data can thus be obtained even for a penetration depth of the order of 50 nm (provided that a proper calibration on Silica reference sample is performed) and the influence of the sub-surface microporosity on the measured elastic modulus and hardness can be estimated. In all cases, the cross-sections of the samples were polished before the indentations by means of diamond lapping films in 15, 6, 3 and 1 microns grades, each for one minute. More details on the procedure are available in ref. [24].

Four-point bending tests were performed on dense and porous prisms (3 × 4 × 50 mm^3) with smoothed angles (45°), according to ASTM C1161-02c standard. Strain gauges (HBM LY41-3/120) were used for strain measurements on dense samples, while inductive sensors were employed for porous materials, in order to avoid any influence of the glue on the mechanical results. The crosshead speed was set at 0.5 mm/min.

In view of preparation and observation of vertical sections by the Focus Ion Beam (FIB), the surfaces were first mirror polished, then etched with Ga+ and sputtered with a thin film of platinum (2 μm) to protect the zones which were not cross-sectioned.

3. Results and discussion

All the pure zirconia suspensions presented a very low viscosity and behaved as a Newtonian fluid, whereas they became pseudoplastic after gelatine or agar addition. The viscosity under a shear rate of 20 s^{-1} was equal to ca. 510 mPa·s, 400 mPa·s and above 900 mPa·s, respectively after gelatine, Fluka and Sigma agar addition. Though these values are under the viscosity limit reported in the literature [15] (1000 mPa·s), the casting with the Fluka agar was rather difficult.

3.1. Dense samples

Green gelatine gel-cast components presented densities of about 2.6 g/cm^3 (43 % of the theoretical value, assumed

to be 6.05 g/cm^3 for zirconia) and SEM-FEG observations showed a well-packed microstructure, quite free from defects such as large pores and voids due to entrapped air bubbles. Dense sintered materials (1550°C, 1 hour) reached about 96 - 97 % of their theoretical densities and showed a fine, homogeneous microstructure (Fig. 2).

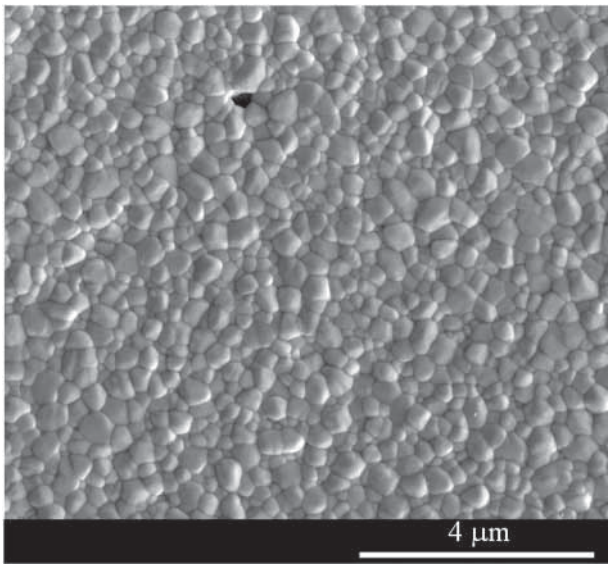

Fig. 2. SEM micrograph of a dense gelatine gel cast ZrO_2 sample.

The results of nanoindentation testing on a 95.5 % dense cylinder are presented in Figs. 3 and 4 and Table 1: no significant variation of the elastic modulus and of the hardness with depth were detected, being values of elastic modulus and hardness in good accordance to the literature.

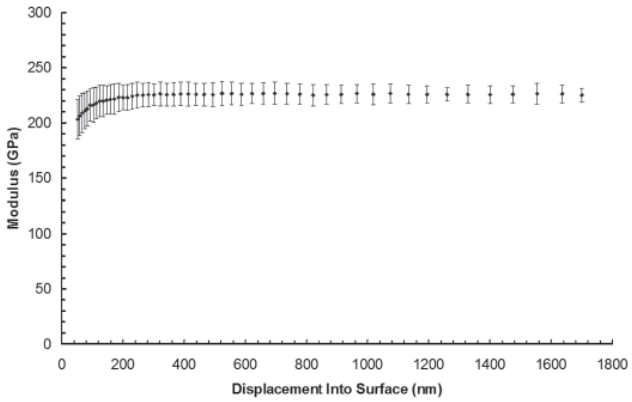

Fig. 3. Elastic modulus in a function of the indenter penetration, assuming a Poisson ratio of 0.3, for a 95.5 % dense gelatine gel cast cylinder (statistical processing of 16 indentations).

Green agar gel-cast components presented densities of 35 ± 0.5 % and 37 ± 4 %, respectively for the Fluka and the Sigma agar. Whatever the agar used, dense samples fired at 1550°C for 1 hour reached a density of 87 ± 1 %. On five bars prepared with the Fluka agar the bending strength was evaluated to 230.0 ± 66.5 MPa and the elastic modulus was 137.8 ± 4.8 GPa. However, due to the fact that in the suspension the solid content was lower respect to the one prepared with the Sigma agar and to its lower purity and the casting difficulties, the use of Fluka agar was abandoned.

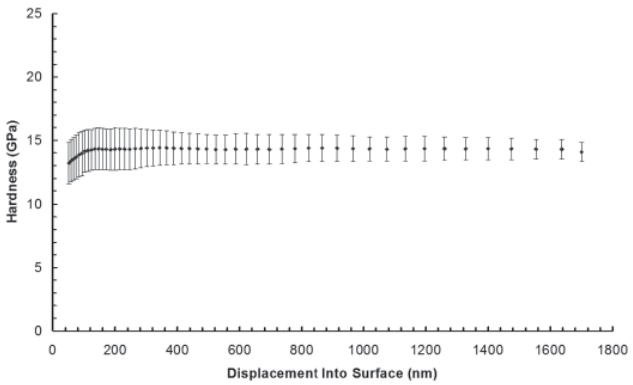

Fig. 4. Hardness in function of the indenter penetration for a 95.5 % dense gelatine gel cast cylinder (statistical processing of 16 indentations).

Table 1. Average hardness and elastic modulus for a 95.5 % dense gelatine gel cast cylinder.

Average hardness [GPa]	Average modulus [GPa]	Depth range considered for averaging [nm]
14.32 ± 1.02	226.11 ± 8.39	400-1500

A 2 hours plateau at 1550°C allowed the geometrical density of the samples to increase up to 93.4 ± 1.2 %. However, the samples prepared with the Sigma agar were characterized by a diffused porosity, which was drastically reduced with a soaking time of 2 hours, as also confirmed by mercury intrusion porosimetry (Table 2).

Table 2. Total porosity and mean pore diameter on samples sintered at 1550°C for one (B65) or two hours (B68) (average of 2 measurements).

Sample	B65	B68
Total porosity [%]	6.8 ± 1.1	0.5 ± 0.3
Mean pore diameter [μm]	7.8 ± 0.6	0.7 ± 0.4

Table 3. reports the flexural strength and the elastic modulus of the dense prisms made from Sigma agar and sintered at 1550°C for 2 hours. The higher density of these samples with respect to the Fluka ones can explain the higher flexural strength. During bending tests, dense material exhibited a perfectly elastic behaviour, and brittle fraction was evidenced by the total absence of plastic deformation: the maximum measured strain was lower than 0.32 % [28].

FEG-SEM observations of a fracture surface of a bar made with the Sigma agar, after the flexural test, revealed submicron grains and small porosities, some of them elongated, of about 2 micron in length (Fig. 5).

On the same sample, mirror polished, 12 nanoindentations in a continuous stiffness measurement mode were done (Table 4, Figs. 6 and 7), to evaluate hardness and

Table 3. Four-point bending tests results on 7 dense samples from Sigma agar.

sflex [MPa]	Ebend [GPa]
413.7 ± 110	170 ± 6.4

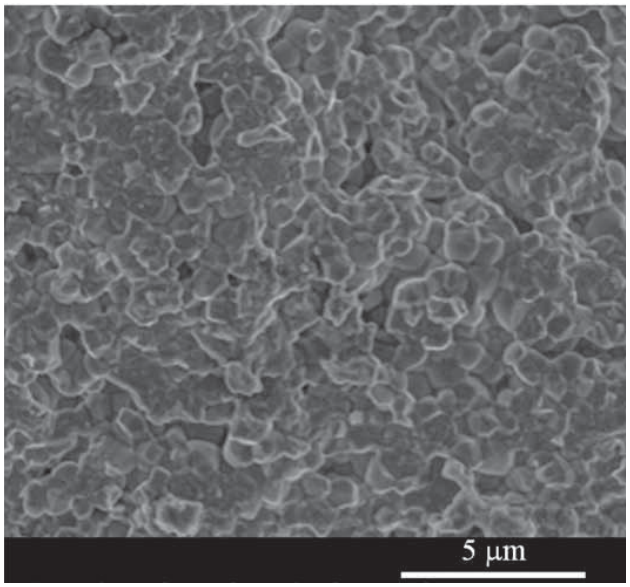

Fig. 5. SEM micrographs of a fracture surface after flexural test.

elastic modulus of the sample. The influence of the diffuse microporosity on elastic modulus and hardness is rather evident in Figs. 6 and 7: these properties are not constant with depth [28].

Table 4. Average hardness and elastic modulus for dense zirconia made from Sigma agar.

Average hardness [GPa]	Average modulus [GPa]	Depth range considered for averaging [nm]
13.85 ± 1.55	207.70 ± 15.10	200 - 1200

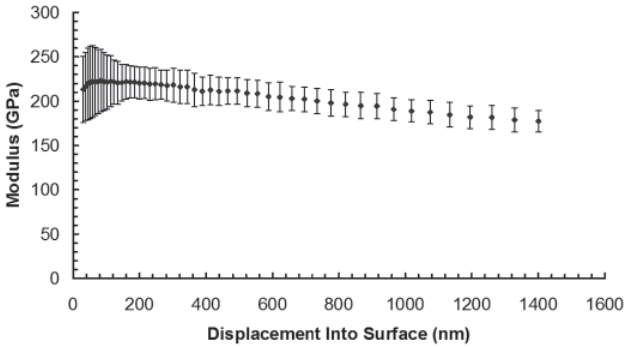

Fig. 6. Elastic modulus in a function of the indenter penetration, assuming a Poisson ratio of 0.3 (statistical processing of 12 indentations).

Hardness and elastic modulus of dense samples prepared with agar were slightly lower with respect to the results obtained with gelatine samples, because of the subsurface porosity, as evidenced by mercury intrusion porosimetry, FIB cross-sectioning and SEM observations.

The measured elastic modulus of the dense samples (170 ± 6.4 GPa) are in the range to those found in the literature (166.8–169.9 GPa) for 7 % porous samples based on a Y-TZP nanopowder with 3 mol.% yttria, according to eq. (4) to (6) [29], where P is the porosity:

$$E = 216 \cdot e^{-3.69P}, \quad (4)$$

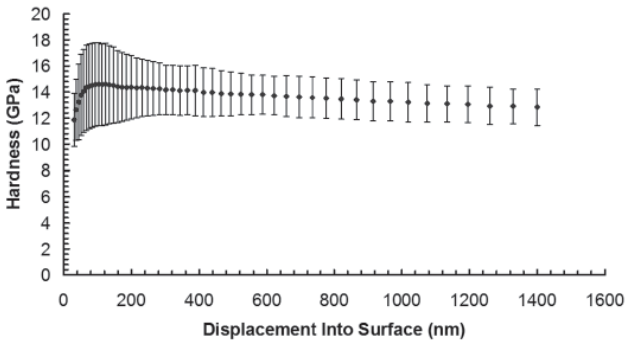

Fig. 7. Hardness in a function of the indenter penetration (statistical processing of 12 indentations).

$$E = 210.6 \cdot (1-P)^{2.96}, \quad (5)$$

$$E = 214.6 \cdot (1-3.3P+3.34P^2). \quad (6)$$

Bending strength is, however, lower (413.7 ± 110 MPa) with respect to ref. [30] for a 10 % porous sample produced by uniaxial compaction and based again on a Y-TZP nanopowder with 3 mol.% yttria, where values of 570 MPa are reported. These results can be explained by the critical defects present in the prepared samples, where elongated pores having 1 to 2 microns in length and a radius curvature in the range 10 - 50 nm were evidenced. Microporosity can be explained by an incomplete agar dissolution and/or because of an insufficient de-airing step [10-11]. In our case, the agar solution was completely clear after 1 hour at 90°C, so, the presence of microporosity is rather due to the lack of de-airing step, though the addition of an antifoaming agent, rather than to an incomplete dissolution of the agar. The slightly gentle evacuation procedure used (tapping) was thus not sufficient to remove the smallest air bubbles from the suspension.

3.2 Porous samples

On P50 porous samples made from gelatine, a micro and a macro porosity were clearly identified in the samples: smaller defects up to 12.6 μm^2 correspond to roughly circular porosities (with a shape factor of ca. 0.89), while macroporosities (up to 200,000 μm^2) have a smaller shape factor (0.252) and are thus less regular objects. These objects are probably due to a non optimal PE spheres dispersion or to non perfectly spherical pore agents within the suspension [24]. On 12 cylinders, fired at 1550°C for 1 hour, with a density of 61.2 ± 2.1 %, a mean compressive strength of 207.4 ± 50 MPa was measured. Concerning compressive tests, though the density values of these samples were rather close, the compressive strength differed significantly among the large samples, without any evident relationship. The presence of defects evidenced by image analysis is probably responsible for the results scattering. On a P50 sample, 59.5 % dense, 12 nanoindentations in a CSM mode were performed (Table 5, Figs. 8 and 9), to evaluate hardness and elastic modulus of the sample.

In this case, the influence of the subsurface porosity is more evident, respect to the dense sample, as elastic modulus and hardness vary slightly with depth.

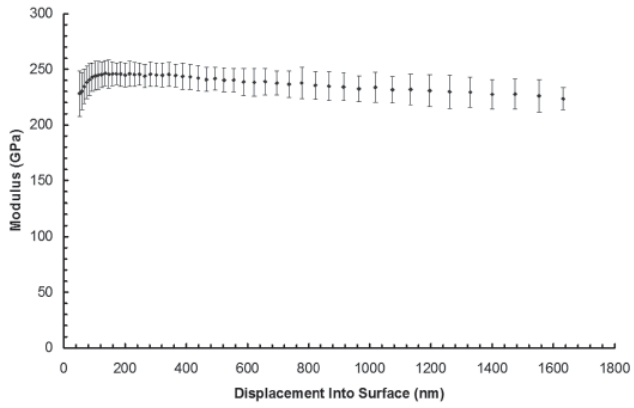

Fig. 8. Elastic modulus in a function of the indenter penetration, assuming a Poisson ratio of 0.3 (statistical processing of 12 indentations).

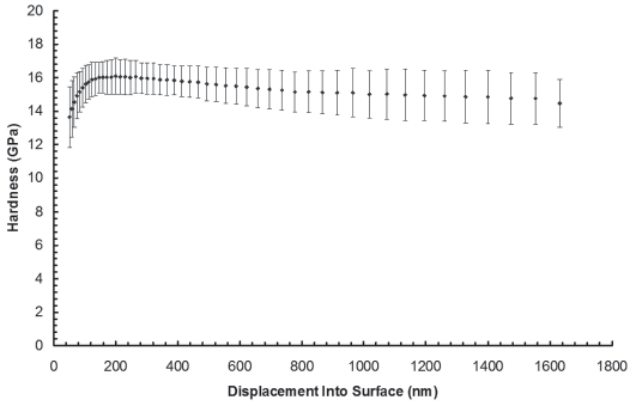

Fig. 9. Hardness in a function of the indenter penetration (statistical processing of 12 indentations).

Table 5. Mean hardness and elastic modulus for porous zirconia (P50) made from gelatine.

Average hardness [GPa]	Average modulus [GPa]	Depth range considered for averaging [nm]
15.26 ± 1.19	235.94 ± 11.65	200 - 1200

The cylindrical porous samples were initially fired at 1550°C for 2 hours, with a heating ramp of 2°C/min. The macropores were rather homogeneously distributed within the ceramic fired material (Fig. 10), both for P50 and P65 samples.

Compressive strength measured on 9 P50 cylinders having a mean density of 63.3 ± 1.5 % was equal to 235.5 ± 79.6 MPa while elastic modulus was equal to 43.3 ± 15.4 GPa.

However, during bars sintering, a two hours plateau at 1360°C was introduced, on the basis of dilatometry results on TZ3-YS powder and the heating rate was also reduced to 1°C/min to avoid deformations. All the samples were then cooled down to room temperature with a cooling rate of 5°C/min. SEM observations revealed that the microstructures obtained with and without the isothermal step at 1360°C were rather similar, as also confirmed by the mercury porosimetry intrusion results (Table 6.). FEG-SEM observations after FIB cross-sectioning confirmed the presence of a diffuse microporosity in the porous bars and cylinders.

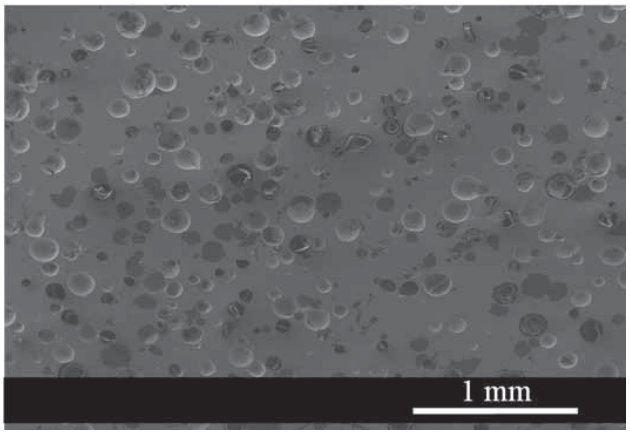

Fig. 10. Representative cross section of a P50 sample.

Table 6. Total porosity and mean pore diameter on P50 samples sintered at 1550°C for two hours, w or w/o isothermal step at 1360°C (average of 2 measurements).

Sample	w/o step	w step at 1360°C
Total porosity [%]	32.9 ± 2.3	36.5 ± 1.6
Mean pore diameter [μm]	1.9 ± 0.6	2.8 ± 0.3

The sintered porous bars presented a geometrical density of 61.6 ± 2.1 % (average value on 13 samples) and 49 ± 1.6 % (average value on 6 samples), respectively for P50 and P65 samples. Table 7. reports the flexural strength and the elastic modulus of the porous bars made from Sigma agar and sintered at 1550°C for 2 hours.

Table 7. Four-points bending tests results on porous bars made from Sigma agar.

	σ flexflex [MPa]	Ebend [GPa]
P50	33.7 ± 11	44 ± 11
P65	12 ± 5	13 ± 8

The dispersion of experimental data was higher than that experienced by dense samples, due to the presence of a much higher number of possible crack origins. The load-deformation curves suggest a different mechanical behavior, deviating from linearity at higher loads and indicating the effect of collapse of the external walls of the macrocells [28].

On a P50 sample (I44) having a density of 62 %, once mirror polished, 12 nanoindentations in a CSM mode were done (Table 8, Figs. 11 and 12).

Table 8. Mean hardness and elastic modulus for porous sample P50 (I44) made from Sigma agar.

Average hardness [GPa]	Average modulus [GPa]	Depth range considered for averaging [nm]
14.8 ± 0.9	211.1 ± 5.4	200 - 1200

SEM observations, after FIB cross-sectioning of a P50 bar (I44), revealed submicronic grains and subsurface porosity having low curvature radii (Fig. 13).

Concerning P50 samples, the average elastic modulus was equal to 44 ± 9 GPa, which was a bit lower respect to

what predicted by the empirical equations (4) to (6), where values ranging from 50.1 to 52.3 GPa are expected. Also the modulus of rupture (33 ± 11 MPa) was lower respect to ref. [30]. These results can be probably explained because when the porosity content increases to a certain level, greater than 25 %, percolation starts and increasingly oblate open pores are formed [29]. Moreover, the used polyethylene spheres are irregular in shape, as already underlined in ref. [24], with respect to the more regular PMMA of ref [30]. Also the size of the polymer beads are rather different: 125 - 300 microns in this work, against 150 - 200 for ref. [30]. The nanoindentation results on sample I44 in Table 8 were rather similar to the ones obtained on dense samples (Table 4) and the influence of the subsurface porosity is again confirmed.

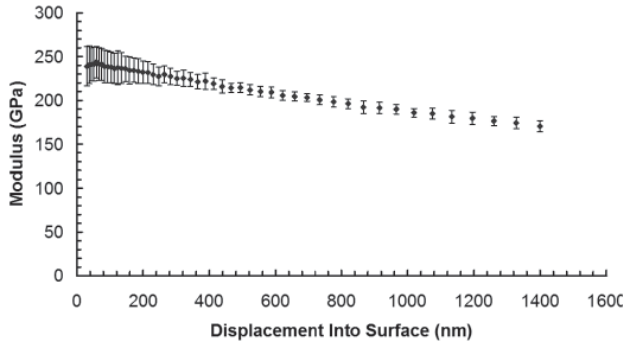

Fig. 11. Elastic modulus in a function of the indenter penetration, assuming a Poisson ratio of 0.3 (statistical processing of 12 indentations).

For macroporous P65 samples the elastic modulus decreases down to 13 GPa (about 7 % of the dense material), and the dispersion of the experimental data is further increased. The mechanism of rupture is not different from that of P50 samples, but the values of modulus of rupture decrease down to 12 MPa, probably indicating the effect of coalescence of macrocavities, and confirming that for very high porosities the thickness of the cell walls becomes unsuitable to guarantee adequate mechanical properties.

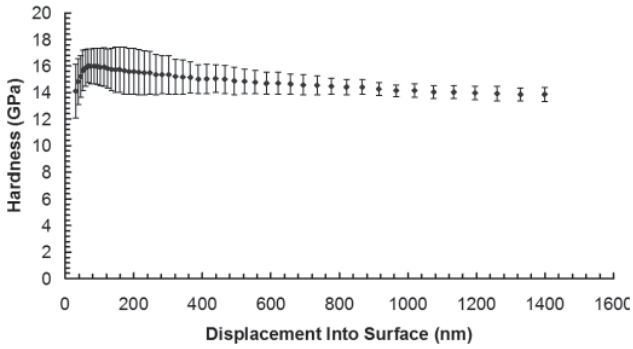

Fig. 12. Hardness in a function of the indenter penetration (statistical processing of 12 indentations).

4. Conclusions

Rather dense and porous 3Y-TZP samples were successfully produced by means of a modified gel-casting process based on gelatine and agar. With gelatine, dense samples were produced but the porous ones presented a non homogeneous distribution of the pores, probably because of a non perfect dispersion within the suspension. On the contrary, with agar, dense samples did not overcome a density of 93.4 ± 1.2 %, in the absence of a de-airing step under vacuum: the addition of an antifoaming agent to the slurries was not sufficient enough to remove all the air bubbles within the suspensions. This microporosity led obviously to a decay of the bending strength and of the elastic modulus. By addition of polyethylene spheres, it was possible to produce around 40-50 vol.% porous samples having a good dispersion of the macropores, thanks to the control of the casting temperature. The flexural strength and the elastic modulus of the porous samples were slightly lower with respect to the data found in the literature, probably because of the residual microporosity and because of the dimensions and the irregularities of the polyethylene beads used.

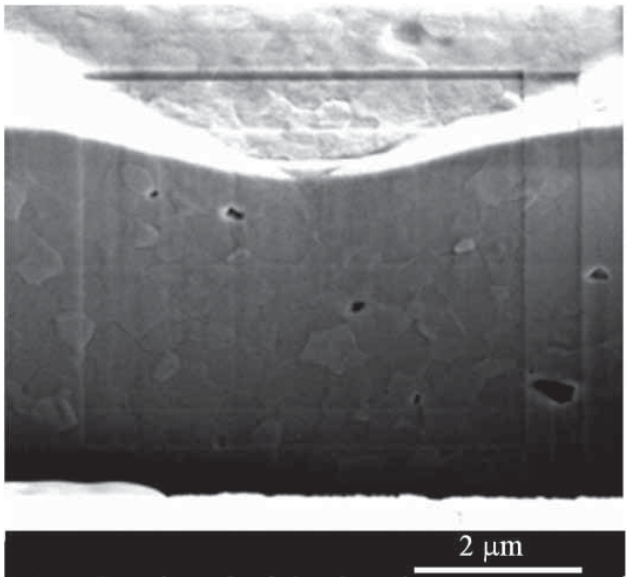

Fig. 13. FEG-SEM micrograph of a porous sample P50 (I44): FIB cross-sectioning of the indented zone.

Acknowledgements

Experimental activities were carried out in the frame of the PRISMA 2005 project “Development of new cellular materials by gel-casting technique: optimization of production process and functional simulation of the microstructure”, INSTM (Inter-University National Consortium on Material Science and Technology), Italy.

References

[1] Studart A.R., Gonzenbach U.T., Tervoort E., Gauckler L.J.: „Processing Routes to Macroporous Ceramics: A Review”, J. Am. Ceram. Soc., 89, (6), (2006), 1771-89.
[2] Colombo P.: „Conventional and novel processing methods for cellular ceramics”, Phil. Trans. R. Soc. A, 364, (2006), 109–24.
[3] Omatete O.O., Janney M.A., Strehlow R.A.: “A new ceramic forming process”, Am. Ceram. Soc. Bull., 70, 10, (1991), 1641-49.
[4] Young A.C., Omatete O.O., Janney, M.A., Menchhofer P.A.,: „Gelcasting of alumina”, J. Am. Ceram. Soc., 74, (1991), 612-8.
[5] Xie Z.P., Yang J.L., Huang D., Chen Y.L., Huang Y.: „Gelation forming of ceramic compacts using agarose” Brit. Ceram. Trans., 98, 2, (1999), 58-61.

[6] Santacruz I., Nieto M.I., Moreno R.: „Alumina bodies with near-to-theoretical density by aqueous gelcasting using concentrated agarose solutions", Ceram. Int., 31, (2005), 439-445.
[7] Millán A.J., Nieto M.I., Moreno R.: „Aqueous injection moulding of silicon nitride", J. Eur. Ceram. Soc., 20, (2000), 2661-2666.
[8] Varma H.K., Sivamukar R.: „Dense hydroxy apatite ceramics through gel-casting technique", Mat. Lett., 29, (1996), 57-61.
[9] Zhang W., Wang H., Jin Z.: „Gel-casting and properties of porous silicon carbide/silicon nitride composite ceramics", Mat. Lett., 59, (2005), 250-256.
[10] Adolfsson E.: „Gelcasting of zirconia using agarose", J. Am. Ceram. Soc., 89, 6, (2006), 1897-1902.
[11] Kong D., Yang H., Wei S., Li D., Wang J.: „Gel-casting without de-airing process using silica sol as a binder", Ceram. Int., 33, (2007) ,133-139.
[12] Sun J., Gao L.: „Influence of forming methods on the microstructure of 3Y-TZP specimens", Ceram. Int., 29, (2003), 971-974.
[13] Millán A.J., Moreno R., Nieto M.I.: „Thermogelling polysaccharides for aqueous gelcasting – part I: a comparative study of gelling additives", J. Eur. Ceram. Soc., 22, (2002), 2223–30.
[14] Dhara S., Bhargava P.: „Egg white as environmentally friendly low – cost binder for gelcasting of ceramics", J. Am. Ceram. Soc., 84, 12, (2001), 3048-50.
[15] Chen Y., Xie Z., Yang J., Huang,Y.: „Alumina casting based on gelation of gelatine", J. Eur. Ceram. Soc., 19, (1999), 271–5.
[16] Vandeperre L.J., De Wilde A.M., Luyten J.: „Gelatin gelcasting of ceramic components", J. Mat. Proc. Tech., 135, (2003), 312-6.
[17] Ortega F.S., Valenzuela F.A.O., Scaracchio C.H., Pandolfelli V.C.: „Alternative gelling agents for the gelcasting of ceramic foams", J. Eur. Ceram. Soc., 23, (2003), 75–80.
[18] Jia Y., Kanno Y., Xie Z.P.: „New gel-casting process for alumina ceramics based on gelation of alginate", J. Eur. Ceram. Soc., 22, (2002), 1911-1916.
[19] Fanelli A.J., Silvers R.D., Frei W.S., Burlew J.V., Marsh G.B.: „New aqueous injection molding process for ceramic powders", J. Am. Ceram. Soc., 72, 10, (1989), 1833-1836.
[20] Sepulveda P.: „Gelcasting foams for porous ceramics", Am. Ceram. Soc. Bull., 76, 10, (1997), 61-65.
[21] Lombardi M., Montanaro L., Grémillard L., Chevalier J.: „New Gelcasting Procedure to Prepare Alumina Porous Components: Process Optimization and Preliminary Mechanical Tests", Proc. 32nd Int. Conf. & Expo. on Advanced Ceramics and Composites, Daytona Beach (FL), USA, (2008).
[22] Tulliani J.M., Naglieri V., Lombardi M., Montanaro L.: „Porous alumina and zirconia bodies obtained by a novel gel-casting process", Proc. 32nd Int. Conf. & Expo. on Advanced Ceramics and Composites, Daytona Beach (FL), USA, (2008).
[23] Lombardi M., Naglieri V., Tulliani J.M., Montanaro L.: „Gelcasting of dense and porous ceramics by using a natural gelatine", J. Porous Mat., 16, 4, (2009), 393-400.
[24] Tulliani J.M., Bartuli C., Bemporad E., Naglieri V., Sebastiani M.: „Preparation and mechanical characterization of dense and porous zirconia produced by gel-casting with gelatin as a gelling agent", Ceram. Int., 35, (2009), 2481-2491.
[25] Oliver W.C., Pharr G.M.: „Review: Measurement of hardness and elastic modulus by instrumented indentation: Advances in understanding and refinements to methodology", J. Mat. Res., 19, 1, (2004), 3-20.
[26] Oliver W.C., Pharr G.M.: „Improved technique for determining hardness and elastic modulus using load and displacement sensing indentation experiments", J. Mat. Res., 7, 6, (1992), 1564-1580.
[27] King R.B.: „Elastic analysis of some punch problems for a layered medium", Int. J. Sol. Struct., 23, 12, (1987), 1657-1664.
[28] Bartuli C., Tulliani J.M., Bemporad E., Tirillò J., Pulci G., Sebastiani M.,: „Mechanical properties of cellular ceramics obtained by gel casting: characterization and modelling", J. Eur. Ceram. Soc., 29, (2009), 2979-2989.
[29] Luo J., Stevens R.: „Porosity-dependence of elastic moduli and hardness of 3Y-TZP ceramics", Ceram. Int., 25, (1999), 281-286.
[30] Gain A.K., Song H.Y., Lee B.T.: „Microstructure and mechanical properties of porous yttria stabilised zirconia ceramic using poly methyl methacrylate powder", Scripta Mat., 54, (2006), 2081-2085.

♦

Received 27 April 2010; accepted 26 May 2010